Cell, Vol. 92, 401–413, February 6, 1998, Copyright ©1998 by Cell Press

TRF2 Protects Human Telomeres from End-to-End Fusions

Bas van Steensel, Agata Smogorzewska, and Titia de Lange*
The Rockefeller University
New York, New York 10021

Summary

The mechanism by which telomeres prevent end-to-end fusion has remained elusive. Here, we show that the human telomeric protein TRF2 plays a key role in the protective activity of telomeres. A dominant negative allele of TRF2 induced end-to-end chromosome fusions detectable in metaphase and anaphase cells. Telomeric DNA persisted at the fusions, demonstrating that TTAGGG repeats per se are not sufficient for telomere integrity. Molecular analysis suggested that the fusions represented ligation of telomeres that have lost their single-stranded G-tails. Therefore, TRF2 may protect chromosome ends by maintaining the correct structure at telomere termini. In addition, expression of mutant forms of TRF2 induced a growth arrest with characteristics of senescence. The results raise the possibility that chromosome end fusions and senescence in primary human cells may be caused by loss by TRF2 from shortened telomeres.

Introduction

Based on genetic and cytological observations, Muller (1938) and McClintock (1941 and 1942) reasoned that telomeres protect chromosomes from end-to-end fusion. Telomeres are now understood to be terminal complexes of repetitive sequences and associated proteins that distinguish natural chromosome ends from damaged DNA. Despite their extensive characterization in yeasts, ciliates, and mammals, the molecular mechanism by which telomeres prevent end-to-end fusions is unclear. Here, we address this issue in human cells by direct visualization of chromosome behavior after interference with the function of a telomeric protein.

Human chromosome ends carry 2–30 kb of double-stranded TTAGGG repeats, which are necessary for telomere function in somatic cells (Farr et al., 1991; Hanish et al., 1994). In the germline and in immortalized cells, this sequence can be maintained by telomerase, a reverse transcriptase that adds TTAGGG repeats onto the 3′ ends of chromosomes (for review, Morin, 1996). The termini of human telomeres carry long (~150 nt) protrusions of single-stranded TTAGGG repeats (Makarov et al., 1997; McElligott and Wellinger, 1997; Wright et al., 1997), which are an effective substrate for telomerase in vitro. According to one analysis (Makarov et al., 1997), G-strand overhangs appear to be present at most chromosome ends and are maintained in cells lacking telomerase, suggesting that a 5′-3′ exonuclease acting on the C-rich telomeric strand may be responsible for their formation. However, other experiments suggest that long G-strand tails are only present on half of the chromosome ends, consistent with their being generated by incomplete lagging-strand synthesis during DNA replication (Wright et al., 1997).

Telomeres in somatic human cells shorten by 50–200 bp per cell division (Cooke and Smith, 1986; Harley et al., 1990; Hastie et al., 1990; reviewed in Harley, 1995). Programmed telomere shortening in normal human cells is probably best viewed as a tumor suppressor mechanism that limits the growth potential of transformed cells (reviewed in de Lange, 1998). In agreement, telomere length is strongly correlated with the proliferative capacity of normal human cells (Allsopp et al., 1992), the catalytic subunit of telomerase (hTRT/hEst2p) is up-regulated in human tumors and immortalized cells (Meyerson et al., 1997; Nakamura et al., 1997), and activation of telomerase in primary human cells results in the extension of cellular life span beyond the scheduled senescence point (Bodnar et al., 1998).

Loss of telomere function in human cells results in the formation of dicentric chromosomes and other abnormalities created through end-to-end fusions (Counter et al., 1992). Both in senescent cells and in tumor cells, dicentric chromosomes, rings, and sister-chromatid fusions are correlated with critically shortened telomeres (reviewed in de Lange, 1995). These observations, taken together with evidence for a protective role of telomeres from yeast, ciliates, flies, and maize, have led to the supposition that chromosome ends lacking telomeric DNA fail to recruit a terminal protein complex required for their protection. However, there has been no direct evidence for telomeric proteins that protect chromosome ends from end-to-end fusion, and it has remained obscure how such factors might act.

Two human telomeric DNA-binding proteins have been identified. TRF1 was isolated as a double-stranded TTAGGG repeat–binding protein from HeLa cells (Chong et al., 1995). This factor is a homodimeric protein with a C-terminal helix-turn helix motif similar to the Myb and homeodomain DNA–binding folds (Bianchi et al., 1997; reviewed in Konig and Rhodes, 1997; Smith and de Lange, 1997). TRF2 carries a similar C-terminal Myb motif but is different from TRF1 in that its N terminus is very basic rather than acidic (Bilaud et al., 1997; Broccoli et al., 1997) (Figure 1). Both proteins bind specifically to double-stranded TTAGGG repeats in vitro and are located at telomeres in vivo. The two TRFs are ubiquitously expressed, and current evidence indicates that most human telomeres contain both factors bound simultaneously throughout the cell cycle (Chong et al., 1995; Broccoli et al., 1997; Smith and de Lange, 1997; van Steensel and de Lange, 1997) (this report, Broccoli, et al., unpublished data). TRF1 was recently inferred to be a negative regulator of telomere length maintenance (van Steensel and de Lange, 1997), because overexpression results in a gradual decline of telomere length, and inhibition of TRF1 generates a telomere elongation phenotype. Here, we document a key role for TRF2 in a second function of telomeres: the protection of chromosome ends from end-to-end fusion.

*To whom correspondence should be addressed.

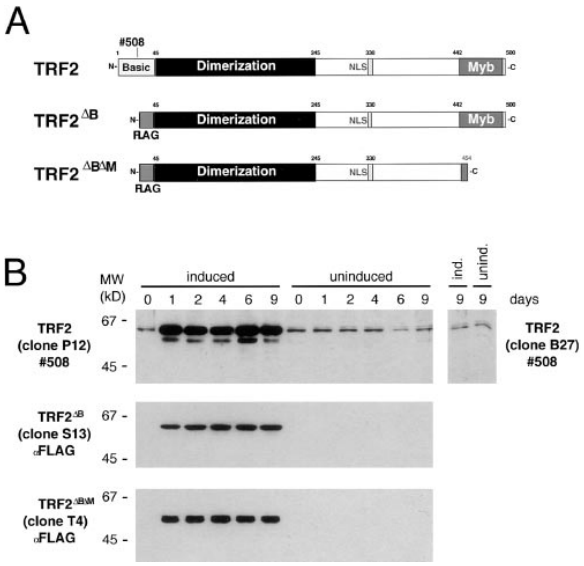

Figure 1. Inducible Expression of TRF2 Proteins in HTC75 Cells

(A) Full-length human TRF2 (Broccoli et al., 1997) and the deletion mutants TRF2$^{\Delta B}$ and TRF2$^{\Delta B\Delta M}$. The approximate position of the peptide used to raise the polyclonal αTRF2 antibody 508 is indicated. The two TRF2 deletion mutants carry an N-terminal FLAG epitope.

(B) Western analysis of the inducible expression of the three forms of TRF2 shown in (A). Whole-cell extracts were prepared from clonal HTC75-derived cell lines expressing the full-length TRF2 (clone P12), TRF2$^{\Delta B}$ (clone S13), TRF2$^{\Delta B\Delta M}$ (clone T4), and control cell line B27, which contains the empty vector. Extracts were prepared from cells grown in parallel in the presence (uninduced) or absence (induced) of doxycyclin for the indicated time. For each extract 20 μg of protein was fractionated, blotted, and incubated with the primary antibodies indicated. TRF1 protein, although present in the extracts, is not detected by the antibodies used. The minor, smaller species detected with antibody 508 probably represent a degradation product of TRF2.

Results

Overexpression and Inhibition of TRF2

To examine the role of TRF2 at human telomeres, we used an inducible expression system based on the cell line HTC75, a tetracyclin-inducible derivative of the human fibrosarcoma cell line HT1080, which was previously employed for the functional analysis of TRF1 (van Steensel and de Lange, 1997). Using this approach, we expressed full-length TRF2 protein and two truncated alleles in a doxycyclin-controlled fashion (see Experimental Procedures). One allele (TRF2$^{\Delta B}$) lacked the N-terminal basic domain, and the second allele (TRF2$^{\Delta B\Delta M}$) also lacked the C-terminal Myb domain (Figure 1A). The two truncated proteins were endowed with an N-terminal FLAG tag allowing their detection with a FLAG-specific monoclonal antibody. For detection of full-length TRF2, a polyclonal antibody directed against aa 16-42 was raised and affinity-purified (antibody 508; see Figure 1). Clonal HTC75 cells transfected with each of the three TRF2 constructs were derived and shown to express appropriately sized TRF2 polypeptides in an inducible manner, with expression reaching plateau levels 1–2 days postinduction (Figure 1B). Expression of the endogenous TRF2 protein was not affected by doxycyclin (Figure 1B). Overexpression of full-length TRF2 was also demonstrated by a gel-shift assay for the detection of TTAGGG repeat–binding activity (data not shown).

Consistent with previous experiments using epitope-tagged protein (Broccoli et al., 1997), endogenous TRF2 protein localized predominantly to telomeres, as evident from the punctate pattern in interphase and the terminal localization of TRF2 signals in many of the metaphase chromosomes (Figures 2A and 2B). Furthermore, most of the TRF2 pattern colocalized with TRF1 in interphase nuclei (Figures 2C and 2D), but further analysis will be required to establish whether all telomeres contain both TRF1 and TRF2 at all times.

Transient overexpression of TRF2 had a mild effect on the localization of TRF1 at telomeres (Figures 2C and 2D, arrowhead), although a strong effect was noted in a few transfected cells with very high levels of TRF2 (Figures 2C and 2D, carets). Similarly to full-length TRF2, TRF2$^{\Delta B}$ accumulated at telomeres (Figure 2E), consistent with previous evidence that the basic domain is not required for the localization of this protein to chromosome ends (Broccoli et al., 1997). Cells expressing high levels of TRF2$^{\Delta B}$ showed diminished levels of the endogenous full-length TRF2 on telomeres, evidencing a weak dominant interfering activity for this allele (Figure 2F). TRF2$^{\Delta B}$ also had a modest effect on the binding of endogenous TRF1 (Figures 2G and 2H; data not shown).

TRF1 binds to telomeric DNA as a homodimer, requiring two Myb domains for stable association with its target site in vitro and in vivo (Bianchi et al., 1997; van Steensel and de Lange, 1997). This architecture has allowed the design of a dominant negative allele of TRF1 containing the dimerization domain and the NLS but lacking the Myb DNA–binding domain (van Steensel and de Lange, 1997). Because TRF2 carried a similar dimerization domain (Broccoli et al., 1997), we asked whether expression of an allele of TRF2 that lacked the Myb motif also acted in a dominant negative fashion. Expression of this version of TRF2 (TRF2$^{\Delta B\Delta M}$, Figure 1A) resulted in a diffuse nuclear staining without evidence for accumulation of this protein at telomeres as expected from the absence of its DNA-binding domain (Figures 2I and 2K). The expression of TRF2$^{\Delta B\Delta M}$ clearly interfered with the accumulation of the endogenous TRF2 protein at telomeres (Figure 2J). Although TRF2 could be readily demonstrated at telomeres in untransfected control cells, little or no TRF2 protein was observed at telomeric sites in cells expressing the TRF2$^{\Delta B\Delta M}$, attesting to the dominant negative activity of this protein. Consistent with the earlier finding that the dimerization domains of TRF1 and TRF2 do not show strong interactions in vitro (Broccoli et al., 1997), TRF2$^{\Delta B\Delta M}$ did not affect the accumulation of the endogenous TRF1 protein on telomeres (Figures 2K and 2L).

TRF2$^{\Delta B\Delta M}$ and TRF2$^{\Delta B}$ Induce a Growth Arrest in HTC75 Cells

Whereas overexpression of full-length TRF2 had no significant effect on the short-term growth of HTC75 cells, induction of TRF2$^{\Delta B\Delta M}$ and TRF2$^{\Delta B}$ led to nearly complete

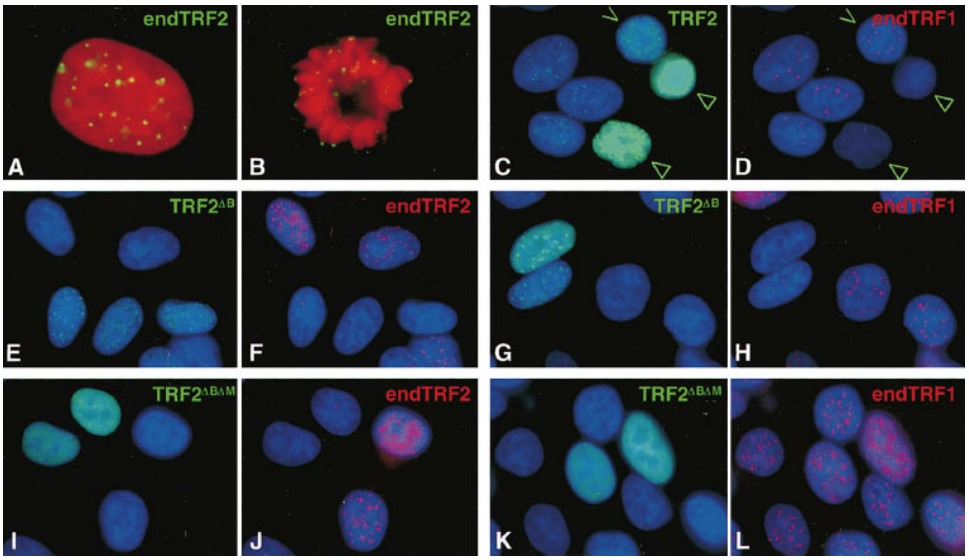

Figure 2. In Vivo Effects of TRF2 Mutants on Telomere Binding of Endogenous Wild-Type TRF1 and TRF2 in Transiently Transfected HeLa Cells

(A and B) Localization of endogenous wild-type TRF2 using antibody 508 (green/yellow) in an interphase nucleus (A) and on mitotic chromosomes (B) of HeLa cells. DNA was stained with DAPI (shown in red).

(C and D) HeLa cells transiently transfected with wild-type TRF2 were dual-labeled for TRF2 using antibody 508 (green in [C]) and endogenous TRF1 using mouse serum 2 (endTRF1, red in [D]). Three transfected cells overexpressing TRF2 are indicated by arrowheads; the other three cells were probably not transfected and showed levels of endogenous TRF2 similar to untransfected control cells.

(E–H) HeLa cells transiently transfected with TRF2$^{\Delta B}$ were dual-labeled for FLAG-tagged mutant protein using antibody M2 (green in [E] and [G]) and either endogenous TRF2 (endTRF2, red in [F]) or endogenous TRF1 (endTRF1, red in [H]).

(I–L) HeLa cells transiently transfected with TRF2$^{\Delta B\Delta M}$ were dual-labeled for FLAG-tagged mutant protein using antibody M2 (green in [I] and [K]) and either endogenous TRF2 (red in [J]) or endogenous TRF1 (red in [L]). DAPI-staining of nuclear DNA in [C]–[L] is shown in blue.

inhibition of proliferation after approximately 4 days of culturing in the absence of doxycyclin (Figure 3A). This growth arrest was accompanied by induction of senescence-associated β-galactosidase (SA-β-Gal) (Dimri et al., 1995; Figure 3B), indicating that the cells were undergoing changes akin to senescence. However, the SA-β-Gal staining of the arrested HTC75 cells was less intense than senescent primary human fibroblasts (data not shown). In addition, the cells became enlarged, had a vacuolated cytoplasm, and often showed multiple small nuclei (Figure 3B), all morphological phenomena associated with senescence of human cells (Hayflick and Moorhead, 1961; Sherwood et al., 1988). Consistent with senescence, the arrest appeared irreversible because addition of doxycyclin to the media (to repress synthesis of the TRF2 mutant proteins) on day 12 did not alter the morphology or the proliferative arrest of the cells over a period of 9 days (data not shown). A substantial proportion of the cells in each culture failed to show convincing morphological alterations and did not express SA-β-Gal (Figure 3B). Most of these cells expressed very low levels of the TRF2 deletion derivatives (data not shown). Collectively, the data suggested that TRF2$^{\Delta B}$ and TRF2$^{\Delta B\Delta M}$ induced a growth arrest with phenotypic characteristics of senescence. The mechanism of this induction and its relationship to senescence in primary human cells is the subject of a separate study.

TRF2$^{\Delta B\Delta M}$ Induces Chromosome End Fusions

Microscopic analysis of DAPI-stained cells expressing TRF2$^{\Delta B\Delta M}$ revealed the frequent occurrence of anaphase bridges and lagging chromosomes (Figure 4A). This phenotype was not observed after induction of control cells not expressing TRF2 proteins or in cells induced for full-length TRF2 or TRF2$^{\Delta B}$ (Figure 4B, and data not shown). We did note, however, that cells expressing TRF2$^{\Delta B}$ often contained small DAPI-positive fragments that were detectable in anaphase (data not shown). The nature of this phenotype is under investigation.

The incidence of anaphase bridges and lagging chromosomes was quantitated in a total of 100 anaphase cells expressing TRF2$^{\Delta B\Delta M}$, uninduced control cells, and in a cell line expressing TRF2$^{\Delta B}$. At day 4 after induction of TRF2$^{\Delta B\Delta M}$, 40% of the cells had one or more aberrant chromosome (a bridge or a lagging chromosome), and the culture showed on average 0.7 fusions per anaphase cell (Figure 4B). By contrast, the level of anaphase bridges and lagging chromosomes was low ($<$0.1 per cell) in the uninduced control cells and in a cell line expressing TRF2$^{\Delta B}$ (Figure 4B).

Chromosome end fusions induced by TRF2$^{\Delta B\Delta M}$ were also detected in metaphase spreads. Colcemid-treated cells showed dicentrics fused at one or both chromatids, multiple-fused chromosomes, and ring chromosomes (Figure 4C, and Table 1). After induction for 6 days, 88% of the metaphases showed at least one fusion (Table 1). Several cells showed trains of 3 or 4 chromosomes (Figure 4C), and one cell showed as many as 30 individual fusion events (data not shown). On average there were 2.4 fusion events per cell in cultures of the T4 clone when induced to express TRF2$^{\Delta B\Delta M}$ for 4 or 6 days. Uninduced T4 cells showed only 0.4 events per cell (Table 1). Similarly, a second cell line (T19) expressing

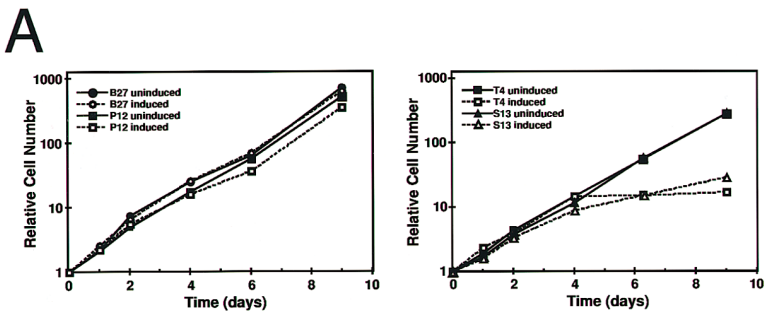

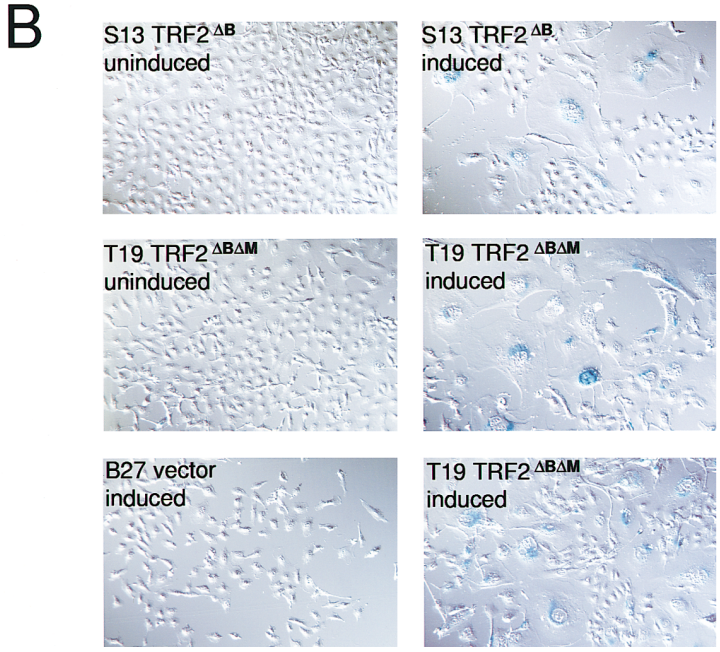

Figure 3. Growth Arrest and Induction of a Senescent Phenotype in Response to TRF2 Mutants

(A) Graphs showing the effect of induction of full-length TRF2 (clone P12), TRF2$^{\Delta B}$ (clone S13), and TRF2$^{\Delta B\Delta M}$ (clone T4) on the growth of HTC75 cells. B27 is a clonal HTC75 cell line containing the vector.

(B) Morphological changes of the indicated HTC75 clones expressing the indicated TRF2 alleles grown for 9 days in the presence or absence (uninduced and induced, respectively) of doxycyclin. Cells were stained for β-galactosidase activity at pH 6.0 and photographed using DIC optics.

TRF2$^{\Delta B\Delta M}$ showed an increase of the fusion frequency from 0.6 to 3.5 per cell upon induction of this dominant negative allele of TRF2. Cells with end-to-end fusions were rare in a control HTC75 cell line transfected with the vector (B27) or in cells expressing TRF2$^{\Delta B}$ (S13) (Table 1). In each case less then 0.3 fusions were observed per cell, and fusions were only seen in 10%–20% of the cells. Some of these apparent fusion events may represent fortuitous juxtaposition of chromosome ends during spreading. Thus, expression of the dominant negative allele of TRF2 increases the frequency of end-to-end fusions by at least 10-fold. The relatively high frequency of end-to-end fusions in the cell lines T4 and T19 in the presence of doxycyclin is probably due to low levels of expression of the TRF2$^{\Delta B\Delta M}$ protein in a fraction of the cells. Such leaky expression was detectable by immunofluorescence (data not shown) but apparently too infrequent to be detectable by Western analysis (Figure 1B).

It should be stressed that the detection of chromosome end fusions in anaphase and metaphase cells likely represents an underestimate of the actual number of events. For instance, in metaphase cells we do not score for sister-chromatid fusions or fusions that have been followed by chromosome breakage, and fusions are only detectable in anaphase cells when a bridge or lagging chromosome results. Thus, our quantitation of chromosome ends fusions probably reflects a minimal estimate of the actual fusion frequency in the cells.

Taken together, the cytogenetic analysis indicated that the removal of TRF2 from telomeres leads to loss of telomeric protection, detectable as end-to-end fusion in anaphase and metaphase chromosomes. It was unlikely that this phenotype was caused by the presence of excess TRF2 protein in the nucleoplasm, because overexpression of full-length TRF2 and TRF2$^{\Delta B}$ similarly resulted in the presence of TRF2 throughout the nucleus, yet induction of anaphase bridges was not noted in such cells (data not shown).

Fused Chromosome Ends Contain Telomeric DNA

Fusion of chromosome ends has been documented in cells containing DNA damage and in cells that have depleted their reservoir of telomeric DNA. In those cases, telomeric DNA is usually not detectable at the site of fusion (Blasco et al., 1997). We therefore asked whether the fusions in response to TRF2$^{\Delta B\Delta M}$ were similarly correlated with loss of telomeric DNA from individual chromosome ends. Using a fluorescein-labeled peptide nucleic acid (PNA) [CCCTAA]$_3$ probe specific for

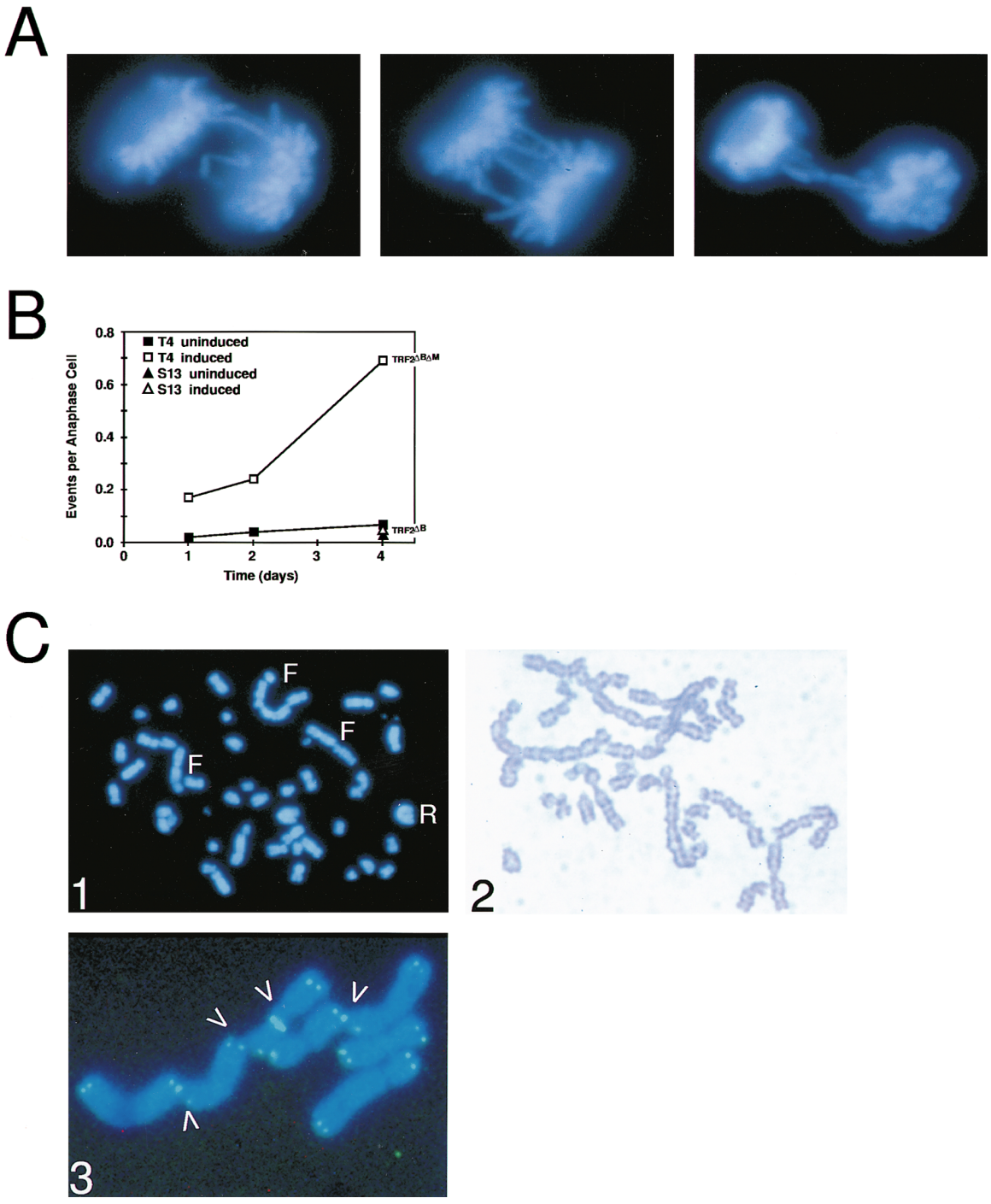

Figure 4. Induction of Anaphase Bridges and Metaphase Fusions by TRF2$^{\Delta B\Delta M}$

(A) Three anaphase cells displaying TRF2$^{\Delta B\Delta M}$-induced anaphase bridges and a lagging chromosome (cell on the left). DNA was stained with DAPI.

(B) Induction of anaphase bridges and lagging chromosomes (together referred to as "events" on the y axis) in T4 cells expressing TRF2$^{\Delta B\Delta M}$ and lack of induced fusions in S13 cells expressing TRF2$^{\Delta B}$. For each time point, one hundred anaphase cells were scored for anaphase bridges and lagging chromosomes.

(C) Telomere fusions in metaphase chromosomes from T4 cells induced to express TRF2$^{\Delta B\Delta M}$. Metaphase chromosomes (1) showing end-to-end fusions stained with DAPI; several fusion events (F) and a ring chromosome (R) are indicated. Metaphase chromosomes G-banded with trypsin (2) showing multiple end-to-end fusions. Detection of telomeric TTAGGG repeats at the sites of telomere fusion (3) (arrowheads). TTAGGG repeats were detected using a fluorescently labeled PNA $[CCCTAA]_3$ probe (green). DNA was stained with DAPI.

telomeric DNA, in situ hybridizations were carried out on metaphase spreads from cells displaying the chromosome ends fusions. The results in Figure 4C showed that telomeric DNA was preserved at the site of chromosome end fusion. In the majority of cases, the signal at the fused ends was substantially stronger than that

Table 1. Induction of Chromosome End Fusions by Mutant TRF2 Proteins

Cell Line	Inducible Gene	Induction	Growth Period (Days)	Number of Cells Examined	Fraction with Fusions	Fusions Per Cell
B27	—	−	4	50	22%	0.2
T4	TRF2$^{\Delta B\Delta M}$	−	4	100	38%	0.4
T4	TRF2$^{\Delta B\Delta M}$	+	4	100	77%	2.4
T4	TRF2$^{\Delta B\Delta M}$	+	6	50	88%	2.4
T19	TRF2$^{\Delta B\Delta M}$	−	4	50	52%	0.6
T19	TRF2$^{\Delta B\Delta M}$	+	4	50	78%	3.5
S13	TRF2$^{\Delta B}$	−	4	50	10%	0.1
S13	TRF2$^{\Delta B}$	+	4	50	20%	0.2

found at free telomeres, consistent with the idea that the telomeric stretches of both fused chromosome ends had remained intact.

TRF2$^{\Delta B\Delta M}$ Induces Molecular Joining of Telomeric DNA Sequences

To establish whether the joining of telomeres in TRF2$^{\Delta B\Delta M}$-expressing cells depended on a proteinaceous bridge, we sought evidence for telomere fusion in naked genomic DNA. Detection of telomeric restriction fragments in genomic DNA from vector control cells and cells expressing full-length TRF2 or TRF2$^{\Delta B}$ showed no change in telomere structure over the course of the induction period (Figures 5A and 5B). By contrast, cells induced for TRF2$^{\Delta B\Delta M}$ revealed a dramatic alteration in the pattern of HinfI/RsaI fragments detectable with TTAGGG-repeat probes (Figure 5B). A new class of longer restriction fragments first became apparent at 4 days postinduction (Figure 5C, and data not shown), and this set of new fragments increased in intensity but not in length over the course of the 9-day experiment. The new class of TTAGGG-repeat fragments was observed in all four independent clonal TRF2$^{\Delta B\Delta M}$ cell lines examined, and in each case they migrated at a MW exactly twice (ratio of 2.0 $\pm$ 0.2 [n = 4]) that of the length of the original population of telomeric fragments. Quantitation of genomic blots indicated that up to 22% (average value 13.8% $\pm$ 6.1% [n = 4]) of the TTAGGG-repeat signal was found in the larger class of hybridizing material at day 9 postinduction.

The fact that the TRF2$^{\Delta B\Delta M}$-induced new TTAGGG-repeat fragments were twice the size of the original telomeres suggested that these molecules might represent the chromosome end fusions that were first detected by cytogenetic analysis of metaphase and anaphase cells. Such structures would be expected to be resistant to exonuclease Bal31 treatment, whereas this exonuclease should readily attack the new class of larger TTAGGG-repeat fragments if they represented elongated telomeres. Bal31 digestion of genomic DNA from T4 cells expressing TRF2$^{\Delta B\Delta M}$ indeed showed the resistance of the longer TTAGGG-repeat fragments to this exonuclease (Figure 5D). Quantitation of a second data set obtained with TRF2$^{\Delta B\Delta M}$-expressing T19 cells (Figure 5E) showed that while the original telomeric loci were gradually shortened by Bal31, the TRF2$^{\Delta B\Delta M}$-induced longer fragments were not affected by the enzyme. This result indicated that the new class of TTAGGG-repeat fragments did not represent elongated telomeres. Most likely, therefore, these longer species are derived from the fused chromosome ends. Because the detection of fused ends in naked DNA argues that the telomeres are held together by nucleic acid interactions, we will refer to these end-joining events as telomeric fusions.

We considered that the telomere fusions might be mediated by (Hoogsteen) base-pairing between the G-strand overhangs at human telomeres. Such a configuration was previously shown to temporarily link the termini of yeast chromosomes, which carry long G tails in late S phase (Wellinger et al., 1993). Because this type of association was shown to be labile at 72°C–78°C, we determined whether the fused human telomeres could be similarly resolved by treatment at that temperature. As shown in Figure 5F, the fused telomeres derived from TRF2$^{\Delta B\Delta M}$-expressing cells are resistant to 85°C and only melt out at higher temperatures that also denature bulk DNA. This observation argues against the presence of G-G basepairing in the 3′ overhang as the main mechanism by which telomere fusions occur. However, it is conceivable that the human G tails form more stable G-G base-paired structures than yeast telomere overhangs. The observation that the fused telomeric fragments are resistant to Bal31 nuclease constitutes further evidence against G-tail interactions in the fused telomeres. Because Bal31 readily cleaves single-stranded DNA, including very short regions of unpaired sequences, such as those occurring due to pyrimidine dimers (Linn and Roberts, 1982), this enzyme would be expected to digest single-stranded regions within G-G base-paired telomeric tails and resolve the joins. Similarly, the telomere fusions were resistant to the single-stranded cleavage activity of mung bean nuclease (data not shown). We therefore favor the idea that the telomere fusions are the result of end-to-end ligations of one or both telomeric strands.

Telomeric Fusions Correlate with the Loss of G-Strand Overhangs

Ligation of telomere termini would be unexpected if, as proposed by Makarov et al. (1997), all or most human telomeres contain long regions of single-stranded TTAGGG-repeat DNA. It was therefore prudent to appraise the status of the telomere termini in cells displaying telomere fusions. Makarov et al. (1997) have developed a method for the quantitative detection of single-stranded TTAGGG repeats at the ends of human chromosomes. In this technique, HinfI/RsaI-digested nondenatured genomic DNA is annealed to labeled $[CCCTAA]_4$ oligonucleotide, and the indirectly labeled

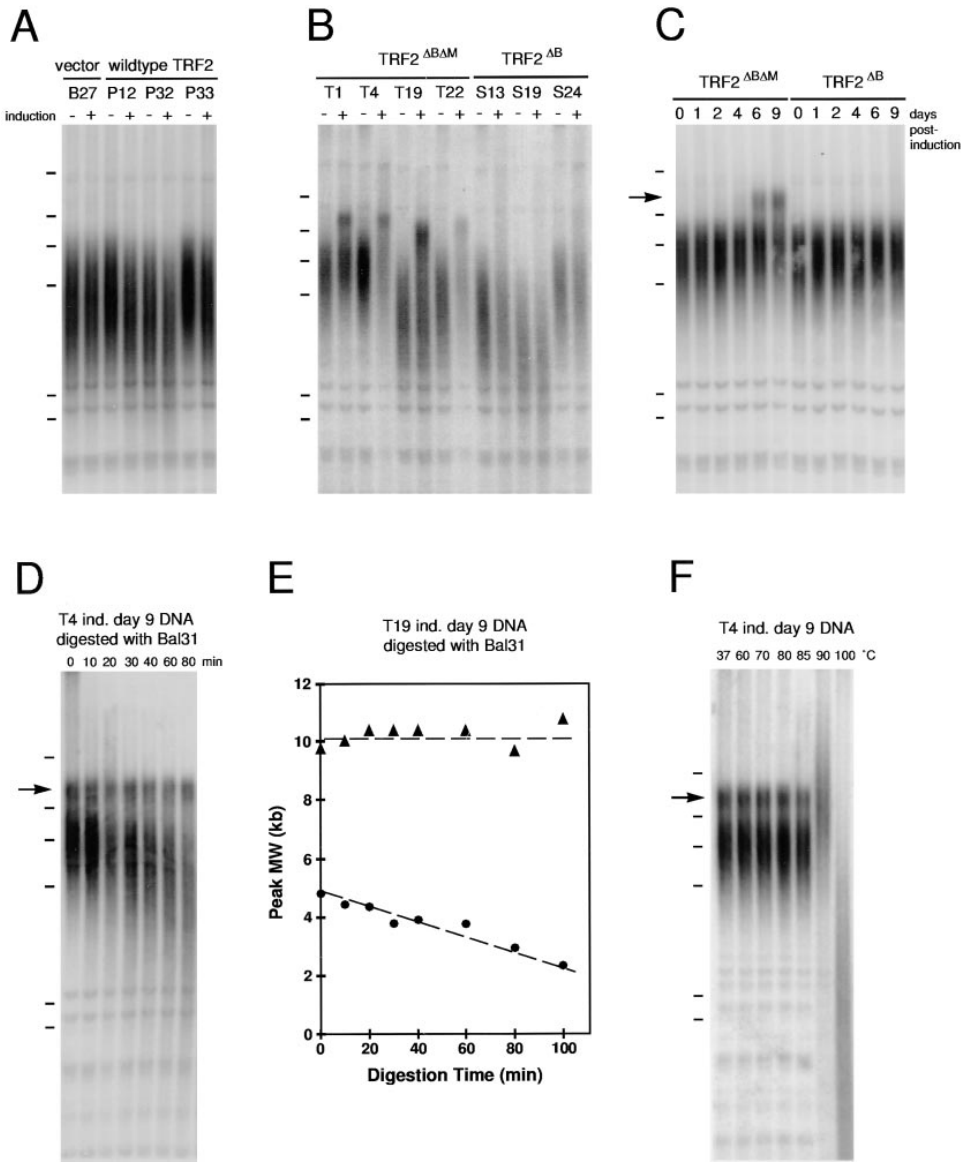

Figure 5. Detection of Telomere Fusions in Naked DNA

(A) Telomere structure in clonal HTC75 lines expressing wild-type TRF2 (P clones) and in a vector control cell line (clone B27) grown in the presence and absence of doxycyclin (− and + induction, respectively) for eight population doublings.

(B) Telomere structure in clonal lines expressing the indicated deletion alleles of TRF2 grown with and without doxycyclin for 9 days (− and + induction, respectively).

(C) Time course of changes in telomere structure in T4 cells induced to express TRF2$^{\Delta B\Delta M}$ and in S24 cells induced to express TRF2$^{\Delta B}$.

(D) Bal31 exonuclease digestion of DNA from T4 cells induced to express TRF2$^{\Delta B\Delta M}$ for 9 days.

(E) Quantitation of a Bal31 exonuclease experiment similar to that shown in (D) performed with DNA from T19 cells induced to express TRF2$^{\Delta B\Delta M}$ for 9 days.

(F) Heat stability of the telomeric fusions. DNA derived from the same cells used in (D) was treated for 10 min at the indicated temperatures and immediately loaded on an agarose gel.

(A–F) All genomic DNA samples were digested with HinfI and RsaI and analyzed by blotting using a TTAGGG repeat–specific probe (see Experimental Procedures). The position of λHindIII DNA marker fragments (23, 9.4, 6.6, 4.4, 2.3, and 2.0 kb) is indicated next to each blot.

telomeric fragments are detected by autoradiography of size-fractionated DNA. With this method it is possible to evaluate the relative amount of unpaired single-stranded TTAGGG repeats in genomic DNA, but the approach does not discriminate between loss of signal due to shortening of the G tails, complete disappearance of G tails, or reduced detection of G tails due to G-G base pairing in the overhangs.

Using the $[CCCTAA]_4$ probe on DNA derived from the control cell line B27, G-strand overhangs at the ends of wild-type telomeres were readily detected (Figure 6). To validate the method, we verified that the probe did not anneal to DNA that was pretreated with mung bean nuclease and that annealing of a $[TTAGGG]_4$ probe did not result in a telomeric pattern (data not shown). When we compared the amount of unpaired TTAGGG-repeat

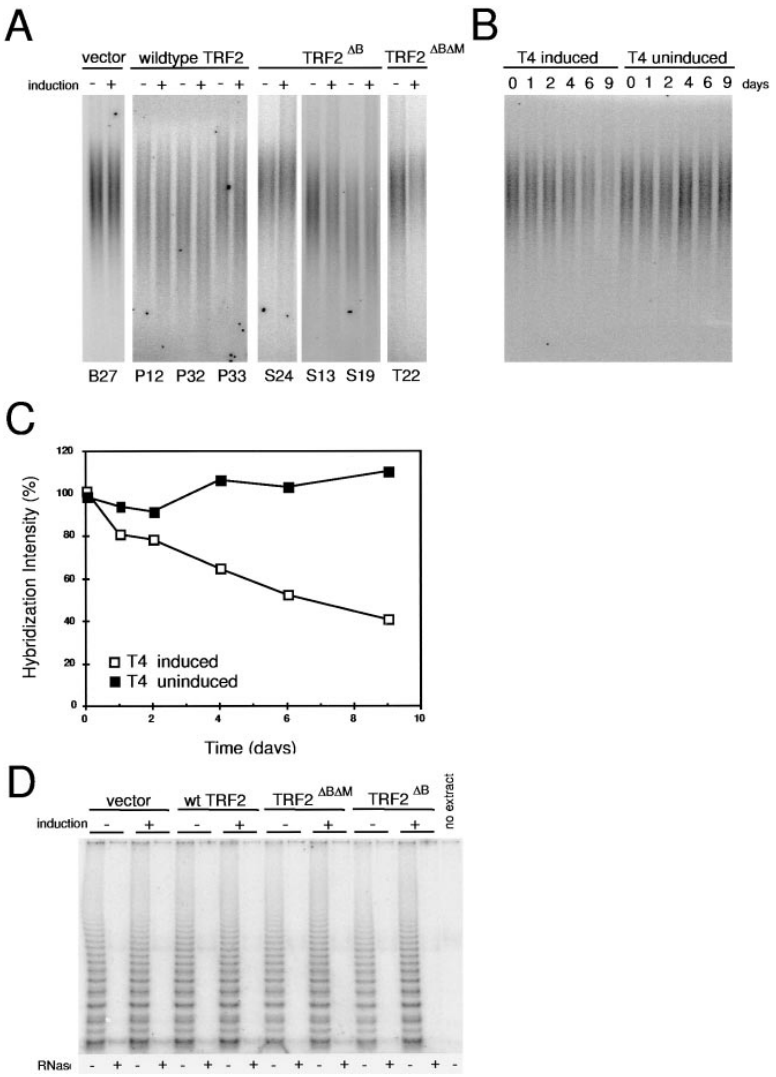

Figure 6. Expression of TRF2$^{\Delta B\Delta M}$ Causes Loss of G-Strand Overhang Signals in the Presence of Telomerase Activity

(A) G-strand overhang assays performed on DNA derived from the indicated cell lines (grown in the presence or absence of doxycyclin for 9 days as indicated) expressing the indicated TRF2 polypeptides.

(B) Time course of the loss of G tails in the T4 clone expressing TRF2$^{\Delta B\Delta M}$.

(C) Quantitation of the loss of G-strand overhangs upon induction of TRF2$^{\Delta B\Delta M}$ in two independents experiments performed with the T4 clone. The data were derived from two experiments similar to those shown in (B), and the average value was plotted.

(D) Similar telomerase activity in four HTC75 clonal lines expressing the indicated TRF2 polypeptides grown for 9 days in the presence or absence of doxycyclin (− and + induction, respectively). For each extract, identical amounts of protein (0.5 μg) were tested using the TRAP assay.

DNA in cells grown in the presence and absence of doxycyclin, no alteration in the signal was noted in three cell lines induced to express full-length TRF2 and three cell lines expressing the TRF2$^{\Delta B}$ allele (Figure 6A). Similarly, overexpression of TRF1 or a dominant negative allele of TRF1 (van Steensel and de Lange, 1997) did not affect the presence of unpaired TTAGGG repeats at telomere termini (data not shown). By contrast, four cell lines expressing TRF2$^{\Delta B\Delta M}$ displayed a consistent reduction in the amount of detectable G-tail sequences, and no signal was present at the position of the larger terminal fragments representing the fused telomeres (Figures 6A and 6B, and data not shown). Quantitation of the data on four clonal cell lines showed that induction of TRF2$^{\Delta B\Delta M}$ for 6–9 days resulted in a 40%–60% decline in the total single-stranded TTAGGG-repeat signals at chromosome ends (Figure 6C, and data not shown). As only 10%–20% of the telomeres have become fused at that time (Figure 5, Table 1, and data not shown), at least some of the loss of the single-stranded G tails in TRF2$^{\Delta B\Delta M}$-expressing cells must have taken place on unfused chromosome ends.

TRF2 Does Not Affect Telomerase Expression

The loss of G-tail sequences in TRF2$^{\Delta B\Delta M}$-expressing cells could be explained if TRF2 is a positive regulator of telomerase expression. We therefore examined the telomerase levels in extracts of cells induced for the three types of TRF2 protein used in this study and matching uninduced controls using the polymerase chain reaction (PCR)–based TRAP assay (Kim et al., 1994). The result revealed similar levels of robust telomerase activity in each cell type regardless of the presence of doxycyclin in the media (Figure 6D), arguing that the telomerase activity is not affected by TRF2 in this setting and that the loss of G-tail DNA occurs through some other mechanism. We note that these results do not address the possibility that TRF2 affects the access of telomerase to telomere termini in vivo.

Discussion

This report defines TRF2 as a human telomeric protein that is required to maintain the correct structure at telomere termini, protects against end-to-end fusions, and

plays a role in successful progression through the cell division cycle. As such, TRF2 appears to be involved in the main functions ascribed to telomeres in somatic human cells and is therefore a likely player in the loss of telomere function and growth arrest that accompanies telomere shortening in normal and transformed human cells.

Telomere Protection by TRF2 and the Role of G Tails

A striking consequence of loss of TRF2 function is the formation of end-to-end fusions detectable in metaphase and anaphase chromosomes. In contrast with the first documented end-to-end fusions, which involved broken chromosome ends in *Drosophila melanogaster* and maize (Muller, 1938; McClintock, 1941; McClintock, 1942), the fusions induced by loss of TRF2 carry telomeric DNA. The presence of telomeric sequences at the fusions was demonstrated by in situ hybridization, and the fused telomeric fragments were detectable in protein-free genomic DNA. Yet while the telomeric TTAGGG repeats persisted, the telomeres failed to protect the chromosome ends from fusion, indicating that the duplex stretch of TTAGGG repeats itself is insufficient for telomere protection in human cells. We conclude therefore that the protective function of telomeres is conferred by a nucleoprotein complex containing TRF2 and possibly other telomeric proteins.

The data also reveal a crucial role for TRF2 in the maintenance of unpaired G-strand overhangs at telomere termini. Loss of TRF2 from telomeres, caused by expression of the dominant negative TRF2$^{\Delta B \Delta M}$ allele, resulted in an approximately 50% reduction in the single-stranded TTAGGG-repeat signal. Although G-G base pairing could be responsible for the diminished detection of the protrusions, we favor the view that inhibition of TRF2 results in an actual loss of G-tail DNA sequences from human chromosome ends. Such G-tail loss could be the consequence of a failure to protect the overhangs from degradation, or it may result from a deficiency in creating new G-tails after DNA replication.

TRF2 is the first telomere-associated protein implicated in the maintenance of the correct DNA configuration of the telomeric 3′ overhang. It was previously shown that telomerase is not involved in the maintenance of G tails in yeast and mammals (Dionne and Wellinger, 1996; Makarov et al., 1997; McElligott and Wellinger, 1997; Wright et al., 1997), and none of the other telomeric proteins identified in eukaryotes are known to affect this aspect of telomere synthesis. Although the mechanism by which TRF2 governs G-tail structure is unclear, our data indicate that changes in telomerase expression are unlikely to be involved in this process.

Collectively, the data are consistent with a model in which TRF2 protects telomeres from fusion through the maintenance of their single-strand TTAGGG-repeat overhangs. This view is consistent with the finding that G-strand overhangs are a universal feature of eukaryotic telomeres (reviewed in Wellinger and Sen, 1997) and identification of G strand–binding proteins in several systems. Thus, one of the main objectives of the transactions at telomeres may be to create and maintain a protrusion of single-stranded telomeric repeats that can bind specific proteins. This terminal complex could constitute the unique aspect of telomeres that allows cells to distinguish natural chromosome ends from broken DNA.

The 3′ extension of TTAGGG repeats at human chromosome ends are likely to serve as a binding site for single strand–specific telomeric proteins, but the actual factors involved in this function are still elusive. A candidate activity that could cap the TTAGGG repeats has been identified in *Xenopus laevis* extracts (Cardenas et al., 1993), G-strand overhangs are bound by terminus-specific proteins in ciliates (Gottschling and Zakian, 1986; Price, 1990), and budding yeast telomeres are protected from degradation by Cdc13p (Garvik et al., 1995), a protein with G tail–binding activity in vitro (Lin and Zakian, 1996; Nugent et al., 1996). However, human homologs of these factors have not been identified yet. It should also be noted that G-rich telomeric repeats have the ability to form G-G (Hoogsteen) base-paired folded structures with several alternative conformations (reviewed by Henderson, 1995) that could potentially contribute to the protection of chromosome ends.

The telomeric fusions are probably the consequence of processing of unmasked telomere termini by enzymes normally acting on broken DNA. A possible scenario is that loss of TRF2 from the chromosome ends leads to disappearance of the G-tail overhangs and activation of a DNA damage response by the denuded telomeres. A cell-cycle arrest might ensue under these conditions, and those cells that process the offending ends into fused telomeres may preferentially continue in the cell cycle leading to the observed metaphase abnormalities and anaphase bridges. The occurrence of fused telomeres in turn creates problems in mitosis due to the mechanical difficulties in segregating dicentric chromosomes, which requires either a break in the spindle or a break in a chromatid. Thus, the loss of telomeric protection may well lead to activation of checkpoints at several stages of the cell cycle. None of these cellular responses to the telomere malfunction induced by TRF2$^{\Delta B \Delta M}$ have been identified so far.

Chromosome End Fusions in Cells with Critically Shortened Telomeres

Telomere associations have been observed by cytogenetic inspection of chromosome behavior in a number of different settings, including senescent primary cells, cells transformed with viral agents, and in a large variety of tumor specimen (reviewed in de Lange, 1995). Although this was not always established in these studies, data accumulated over the past decade suggest that in most cases where telomere associations were observed, the telomeres may have been fairly short. Indeed, in studies that measured telomere length directly, there is a correlation between shortened telomeres and their association in metaphase (Counter et al., 1992; Saltman et al., 1993). Our observations on the behavior of chromosome ends after loss of the duplex telomeric DNA-binding protein, TRF2, now suggest a molecular mechanism underlying these telomere associations. We propose that when the telomeres reach a critical minimal

length their ability to recruit sufficient TRF2 is diminished and end-to-end fusions result. The length setting at which this aspect of telomere function becomes compromised is not yet clear.

Telomeres and Cellular Senescence

Expression of two mutant TRF2 polypeptides induced a growth arrest in the human fibrosarcoma cells used in this study. This arrest had several features consistent with the induction of senescence, including a specific cellular morphology, expression of a β-galactosidase activity correlated with senescence, and the irreversible nature of the arrest. Further analysis will be required to establish whether this senescent-like phenotype in these transformed cells is actually directly related to the replicative senescence described in primary human cells. Regardless of the exact nature of this phenotype, the results indicate that transformed human cells are rather sensitive to the status of their telomeres and that interference with telomere function could inhibit proliferation of malignant cells.

Two mechanisms for the induction of the observed growth arrest can be entertained at this stage. Because the growth arrest in HTC75 cells is accompanied by chromosomal abnormalities, one possibility is that the arrest is a response to DNA damage arising from the altered TRF2 activity at telomeres. The second possibility is that a specific pathway exists allowing cells to evaluate the status of their telomeres. For instance, the presence of the basic N terminus of TRF2 on telomeres may be required to suppress cellular senescence. Overexpression of a mutant protein lacking this domain would then be expected to induce arrest by displacing the endogenous TRF2. Similarly, the strong dominant negative activity of TRF2$^{\Delta B \Delta M}$ would result in telomeres lacking the basic N-terminal domain of TRF2 and cause an arrest signal. Such a mechanism would allow cells to monitor the length of their telomeres and initiate a growth arrest and senescence program in response to critical shortening of the telomeres.

Requirements for Telomere Formation in Human Cells

Transfection of TTAGGG repeats into human cells leads to efficient de novo formation of fully functional telomeres (Farr et al., 1991). We have previously found an excellent correlation between the binding specificity of TRF1 and the *cis*-acting requirements for de novo telomere formation in human cells (Hanish et al., 1994), suggesting that the acquisition of TRF1 might be an essential step in telomere healing. However, the subsequent cloning of TRF2 revealed that this protein has the same sequence preference as TRF1 (Broccoli et al., 1997), raising the possibility that TRF2 rather than TRF1 is involved in the conversion of the transfected DNA into a functional telomere. The finding that TRF2 is important for the protection of chromosome ends now hints at a likely scenario for de novo telomere formation in human cells. Acquisition of TRF2 may be one of the early steps as the transfected telomere seed enters the nucleus. According to the current data, TRF2 has the ability to protect the TTAGGG repeats from ligation to other DNA.

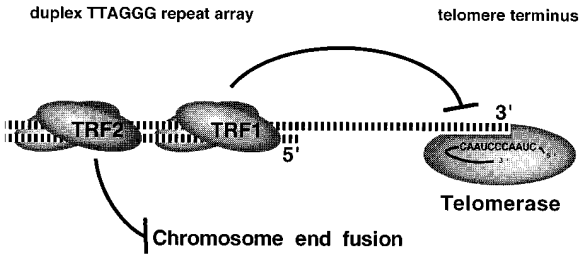

Figure 7. The Role of Human Telomeric Proteins in Telomere Protection and Telomere Length Regulation

TRF1 is depicted as a negative regulator of telomere maintenance, proposed to act by inhibiting telomerase at individual chromosome ends (van Steensel and de Lange, 1997). TRF2 is involved in the protection of chromosome ends by inhibiting end-to-end fusions (this report). Thus, in the process of adding TTAGGG repeats, telomerase synthesizes binding sites for two proteins onto chromosome ends, one of which ensures telomere integrity and the other regulates the length of the telomeres. The relative position and abundance of TRF1 and TRF2 on human telomeres is not known.

As a result, the TRF2-bound end of the transfected linear plasmid may be prevented from undergoing the recombination reaction that normally leads to chromosome-internal integration of transfected DNA. Recombination of the other (nontelomeric) end of the transfected DNA with a resident chromosomal locus will then lead to the observed chromosome fragmentation. Telomerase subsequently elongates the telomere seed to form a fully functional telomere.

Mechanisms of Telomere Function

A general view of the logic underlying the function of human telomeres is now emerging (Figure 7). Human telomerase has long been understood to maintain the terminal sequences of human chromosome ends and thus counter DNA attrition with cell divisions. The need for telomere length maintenance is particularly obvious in immortalized cells and in the germline. However, the current results reveal a second function for telomerase. In addition to balancing the terminal sequence loss that accompanies DNA replication, telomerase actually ensures the continued presence of TRF2-binding sites at chromosome ends by synthesizing arrays of TTAGGG repeats. Because TRF2 is required to prevent telomere fusions, telomerase thus maintains the protective activity of telomeres by constantly replenishing TRF2-binding sites that are lost from telomere termini with DNA replication. This second function of telomerase critically depends on the sequence of the telomeric repeats it synthesizes, and this view predicts that the exact sequence of the telomerase products is a key aspect of the mechanism of telomere function.

In this regard, mutations of the telomerase template RNA in *Tetrahymena thermophila* has given rise to dramatic cellular phenotypes (Yu et al., 1990; Kirk et al., 1997), including occasional anaphase bridges that may well represent telomere fusions of the type reported here. *Tetrahymena* telomeric-binding proteins that could have been displaced by the altered telomeric repeats have not yet been identified. It will be of interest to correlate the effects of altering the telomerase template

sequence in mammalian cells (for example, Marusic et al., 1997) with the binding specificity of TRF2.

Addition of TTAGGG repeats to chromosome ends also ensures the binding of a second telomeric protein, TRF1, that is proposed to act as a negative regulator of telomerase, modulating the length of the TTAGGG repeats arrays at chromosome ends (van Steensel and de Lange, 1997). Thus, the telomerase-mediated maintenance of telomeric TTAGGG repeats secures a functional and regulated telomeric complex required for the integrity of chromosome ends.

Experimental Procedures

Expression Vectors

The cDNA encoding full-length human TRF2 was placed under the tetracyclin-controlled promoter by cloning the EcoRI fragment of plasmid phTRF216-1 (Broccoli, 1997) into vector pUHD10-3, resulting in plasmid pTethTRF2. To facilitate the creation of constructs encoding truncated proteins with an N-terminal FLAG tag, expression vector pTetNFLAG was constructed by inserting a linker encoding a FLAG tag and an EcoRI site into the SacII and BamHI sites of pUHD10-3. Next, TRF2$^{\Delta B}$ (containing aa 45-500) and TRF2$^{\Delta B\Delta M}$ (containing aa 45-454) were each cloned into the EcoRI and BamHI sites of pTetNFLAG (in-frame with the FLAG-tag) by PCR cloning, using Pfu-polymerase, plasmid phTRF216-1 as template, with 5′TTG AATTCGAGGCACGGCTGGAAGAG3′ as forward primer for both constructs, 5′CGGGATCCTGTTTCAGTTCATGCCAA3′ as backward primer for TRF2$^{45\text{-}500}$, and 5′CGGGATCCTCATTCTACAGTCCACTTC TGCT3′ as backward primer for TRF2$^{45\text{-}454}$.

Induction of TRF2 Polypeptides in HTC75 Cells

The empty vector pUHD10-3 and the pUHD10-3-derived constructs for expression of the TRF2 alleles were each cotransfected with neomycin resistance plasmid pNY-HI (H. Tommerup and T. d. L., unpublished data) into cell line HTC75 using the calcium phosphate coprecipitation. HTC75 is a hygromycin-resistant HT1080-derived clonal cell line that stably expresses the tetracyclin-controlled transactivator (tTA) (Gossen and Bujard, 1992; van Steensel and de Lange, 1997). Transfected cells were grown in the presence of doxycyclin (100 ng/ml) and G418 (600 μg/ml). For each construct, approximately 25 G418-resistant cell lines were isolated by ring cloning and tested for expression of TRF2 polypeptides after 24 hr of induction by omission of doxycyclin from the media (doxycyclin acts as a repressor of gene expression in this system). Expression of TRF2$^{\Delta B\Delta M}$ and TRF2$^{\Delta B}$ were tested by immunofluorescence microscopy and western blotting using anti-FLAG antibody M2 (Eastman Kodak); expression of wild-type TRF2 was tested by gelshift assays using a TTAGGG-repeat probe and by western blotting using affinity-purified serum 508 (see below). All clones were grown in DMEM supplemented with 10% bovine calf serum or bovine fetal serum and 150 μg G418 per ml. All clones were grown in parallel with or without doxycyclin (100 ng/ml).

Polyclonal Antibody against TRF2

A 28-*mer* peptide (pep28) encompassing amino acid residues 16-42 of human TRF2 with an additional N-terminal cysteine was synthesized (BioSynthesis, Lewisville, TX) and conjugated to maleimide-activated keyhole limpet haemocyanin (KLH, Pierce, Rockford, IL). Serum from a rabbit immunized with the pep28-KLH conjugate was affinity-purified against pep28 cross-linked to SulfoLink coupling gel (Pierce) using standard procedures (Harlow and Lane, 1988). The resulting purified antibody 508 reacts specifically with TRF2 in western blotting and immunofluorescence labeling assays. The antibody does not cross-react with TRF1 (data not shown).

Whole-Cell Extracts

Cells grown in 10 cm dishes were washed with 5 ml cold phosphate-buffered saline (PBS), harvested by scraping in 1 ml PBS per dish, and centrifuged 2 min in an Eppendorf microfuge at setting 4,000 g. Subsequent steps were all carried out on ice or at 4°C. The cell pellets (~4 million cells) were resuspended in 200 μl buffer C (20 mM Hepes-KOH [pH 7.9], 420 mM KCl, 25% glycerol, 0.1 mM EDTA, 5 mM $MgCl_2$, 1 mM dithiothreitol, 0.5 mM phenylmethylsulfonyl fluoride, 0.2% Nonidet P-40, 1 μg leupeptin per ml, 1 μg pepstatin per ml, 1 μg aprotinin per ml), incubated for 30 min and centrifuged for 10 min in an Eppendorf microfuge at 14,000 g. The supernatant was dialyzed 2–5 hr against 100 ml of buffer D (20 mM Hepes-KOH [pH 7.9], 100 mM KCl, 20% glycerol, 0.2 mM EDTA, 0.2 mM EGTA, 0.5 mM dithiothreitol, 0.5 mM phenylmethylsulfonyl fluoride), frozen in liquid nitrogen, and stored at −80°C. Protein content of the extracts was measured using the Bradford assay (BioRad, Hercules, CA) and using bovine serum albumin as a standard.

Western Blotting

Twenty micrograms of whole-cell extract proteins were separated on 10% SDS-polyacrylamide gels and transferred to nitrocellulose by electroblotting. Ponceau S–staining confirmed equal loading of the samples. Blots were preincubated 30 min in 10% nonfat milk powder and 0.5% Tween-20 in PBS. All subsequent incubations and washing steps were carried out in 0.1% nonfat dry milk powder and 0.1% (w/v) Tween-20 in PBS. Blots were incubated for 12–16 hr at 4°C with either anti-FLAG antibody M2 or anti-TRF2 antibody 508, followed by three 10 min washing steps. Next, blots were incubated 45 min with horseradish peroxidase conjugated sheep-anti-mouse (Jackson) or donkey-anti-rabbit antibody (Amersham) and washed three times for 10 min. Bound antibody was detected using the enhanced chemiluminescence kit (Amersham).

Immunofluorescence Labeling and Microscopy

The HeLaI.2.11 cell line, a subclone of HeLaI (Saltman et al., 1993) bearing telomeres of more than 25 kb (data not shown), was transfected by electroporation with pTethTRF2, pTetFLAGhTRF2$^{\Delta B}$, or pTetFLAGhTRF2$^{\Delta B\Delta M}$ together with the tTA-expression vector pUHD15-1 (Gossen and Bujard, 1992). Cells were grown for 24 hr on Alcian blue–coated coverslips in the absence of doxycyclin. Fixation and immunostaining were carried out as described (Chong et al., 1995; van Steensel and de Lange, 1997). TRF2 was detected with polyclonal antibody 508 (see above), raised, and affinity-purified against an N-terminal peptide of TRF2. The FLAG-epitope tag was detected with the M2 anti-FLAG monoclonal antibody (Eastman Kodak). TRF1 was detected with a mouse polyclonal serum (#2) directed against the full-length protein (S. Smith and T. d. L., unpublished data) or with antibody 371C2 (van Steensel and de Lange, 1997). Rabbit antibodies were detected with fluorescein isothiocyanate (FITC)– or Cy3-conjugated donkey-anti-rabbit antibodies (Jackson ImmunoResearch). Mouse antibodies were detected with FITC-conjugated donkey-anti-mouse antibody (Jackson). Control experiments indicated that secondary antibodies did not show any cross-reaction (data not shown). To exclude that binding of anti-TRF1 (371C2) (van Steensel and de Lange, 1997) and anti-TRF2 (508) antibodies to endogenous TRF proteins was prevented by anti-FLAG antibody M2 through steric hindrance, we preincubated the cells overnight with 371C2 or 508 before adding M2.

Micrographs were recorded on a Zeiss Axioplan microscope with a Kodak DCS200 digital camera. Images were noise-filtered, corrected for background, and merged using Adobe Photoshop.

Cell Growth Curves and β-Galactosidase Assay

Cells were plated in duplicate at various densities (~0.1–4.0 × 10^6 cells/15 cm dish) the day before the experiment. On day 0, all plates were washed three times with medium containing G418 (150 μg/ml) with or without doxycyclin (100 ng/ml). On indicated days, cells were harvested and counted, and cell pellets were frozen at −80°C for isolation of genomic DNA. Whole-cell extracts were prepared from dishes grown in parallel. In most experiments, cells were split at day 4 (1:32–1:4) for day 6 and day 9 time points.

Cells induced for 9 days were stained for β-galactosidase using the method described in Dimri et al. (1995) but with phosphate buffer instead of citrate/phosphate buffer. Cells were washed in PBS (pH 7.2), fixed for 5 min in 2% formaldehyde/0.2% glutaraldehyde solution in PBS , washed again in PBS (pH 7.2), and stained with X-gal (1 mg/ml) in 150 mM NaCl, 2 mM $MgCl_2$, 5 mM $K_3Fe(CN)_6$, 5 mM

$K_4Fe(CN)_6$, and 40 mM NaPi (pH 6.0, pH 4.0 or pH 7.0) for 6–12 hr at 37°C.

Chromosome Analysis in Metaphase and Anaphase Cells

Four to six days after induction (as indicated in the text) cells were incubated with 0.1 μg demecolcine per ml for 90 min, harvested by trypsinization, incubated for 7 min at 37°C in 0.075 M KCl, and fixed in freshly prepared methanol:glacial acidic acid (3:1 vol/vol). Cells were stored at 4°C and when needed dropped onto wet slides and air-dried.

For DAPI staining of DNA, slides with metaphase spreads were incubated 10 min in 0.5 μg 4', 6-diamino-2-phenylindole (DAPI) (Sigma) per ml PBS, washed for 2 min in PBS, and mounted in 90% glycerol/10% PBS containing 1 mg p-phenylene diamine (Sigma)/ml.

For trypsin banding, metaphase spreads prepared as above were incubated in banding solution (2× trypsin-EDTA (Gibco), 1× Hanks Balanced Salt Solution [Gibco] in water) for 45–75 s at 37°C and stained with filtered staining solution (16% Giemsa blood staining solution [J.T. Baker], 4% Giemsa solution [Fisher] in Tris-Maleic acid buffer [pH 5.6]) for 60–75 s at room temperature.

Anaphase cells were visualized by DAPI staining of cells grown on coverslips for the indicated number of days in the presence or absence of doxycyclin.

FISH

In situ hybridization was executed according to Lansdorp et al. (1996). Hybridization was performed with 0.5 μg/ml FITC-conjugated$(C_3TA_2)_3$ PNA probe (Biotech GmbH), and after washing, the cells were embedded in 90% glycerol/10% PBS containing 1 mg p-phenylene diamine (Sigma) per ml, supplemented with 0.2 μg 4',6-diamino-2-phenylindole (DAPI) per ml.

Genomic Blotting and Bal31 Digestion

Isolation of genomic DNA, genomic blotting, and telomere-length estimation were carried out as described (van Steensel and de Lange, 1997). For the Bal31 nuclease experiment, about 65 μg undigested genomic DNA was incubated at 30°C with 13 U Bal31 nuclease (mixed, New England Biolabs, Beverly, MA) in 390 μl buffer containing 600 mM NaCl, 12 mM $CaCl_2$, 12 mM $MgCl_2$, 20 mM Tris-HCl, 1 mM EDTA (pH 8.0). At indicated time points, 30 μl samples were taken and inactivated by addition of 2 μl 0.5 M EGTA and incubation for 10 min at 65°C. Bal31-treated DNA samples were extracted with phenol/chloroform, precipitated with ethanol, and digested with HinfI and RsaI. To ensure equal loading on agarose gels, all DNA samples were quantified after restriction enzyme digestion by fluorometry using Hoechst 33258 dye.

G-Strand Overhang Assay

The nondenaturing hybridization assay to detect G-strand overhangs was carried out essentially as described (Makarov et al., 1997). $[TTAGGG]_4$ and $[CCCTAA]_4$ oligonucleotide probes were end-labeled using γ-^{32}P-ATP (3000 Ci/mmol, Amersham) and T4 polynucleotide kinase. Depending on the experiment, 2.5–5.0 μg HinfI/RsaI digested genomic DNA was ethanol-precipitated, resuspended in 21 μl hybridization buffer (50 mM Tris-HCl [pH 8.0], 50 mM NaCl, 1 mM EDTA), added to 4 μl labeled probe (8 nM), and incubated 10–16 hr at 50°C in a Perkin-Elmer PCR thermocycler. Hybridized samples were size-fractionated on 0.8% agarose gels in 1 × TAE. The gels were dried on Whatman DE-81 filter paper and exposed to autoradiography film or a PhosphorImager screen. As a control, 4 μg HinfI/RsaI-digested DNA was treated for 30 min at 30°C with 0, 10, or 40 U mung bean nuclease (New England Biolabs) in MB buffer (50 mM sodium acetate, 30 mM NaCl, 1 mM $ZnSO_4$ [pH 5.0]), inactivated by addition of 0.01% SDS, and ethanol-precipitated before carrying out the overhang assay. Inspection of the ethidium bromide–stained gel confirmed that mung bean nuclease did not have any detectable endonuclease activity. Treatment with 40 U of mung bean nuclease completely abolished the overhang signal. Annealing with a $[TTAGGG]_4$ probe did not reveal a signal at the position of the telomeres. For quantitation of the G-strand overhangs, hybridization intensity was measured using ImageQuant software by integration of the signal of the entire lane between approximately 1.5–30 kb. DNA samples from cells grown with or without doxycyclin were always analyzed in parallel and run on the same gel.

TRAP Assay

Reactions were performed with whole-cell extracts as described elsewhere (Broccoli et al., 1995). Protein concentrations in the extracts were determined by Bradford assay (BioRad), and 0.5 μg protein was used per extract. RNase digestions were done in parallel to the untreated reaction by addition of 0.2 μg DNase-free RNAse A to the telomerase extension reaction.

Acknowledgments

We are grateful to Peter Lansdorp for technical advice on PNA FISH, to Klaus Damm (Boehringer Ingleheim) for a gift of the PNA probe, to Jim Hudspeth (Rockefeller University) for microscopy facilities, to Susan Smith for the mouse anti-TRF1 antibody, to Matthias Schäfer for preparation of antibody 371C2, to Loretta Grande (New York Hospital) for instruction in G-banding, and to Carolyn Price (University of Nebraska), Ginger Zakian (Princeton University), Mundy Wellinger (University of Sherbrooke), Kiki Broccoli, and Jan Karlseder for helpful discussion. This work was supported by grants from the National Institutes of Health and the Rita Allen Foundation to T. d. L. and a Human Frontier Science Project fellowship to B. v. S.; A. S. is supported by National Institutes of Health Medical Scientist Training Program grant GM07739 to the Cornell/Rockefeller/Memorial Sloan-Kettering Tri-Institutional MD/PhD program.

Received December 3, 1997; revised, January 5, 1998.

References

Allsopp, R., Vaziri, H., Patterson, C., Goldstein, S., Younglai, E., Futcher, B., Greider, C.W., and Harley, C.B. (1992). Telomere length predicts replicative capacity of human fibroblasts. Proc. Natl. Acad. Sci. USA *89*, 10114–10118.

Bianchi, A., Smith, S., Chong, L., Elias, P., and de Lange, T. (1997). TRF1 is a dimer and bends telomeric DNA. EMBO J. *16*, 1785–1794.

Bilaud, T., Brun, C., Ancelin, K., Koering, C.E., Laroche, T., and Gilson, E. (1997). Telomeric localization of TRF2, a novel human telobox protein. Nature Genet. *17*, 236–239.

Blasco, M.A., Lee, H.-W., Hande, M.P., Samper, E., Lansdorp, P.M., DePinho, R.A., and Greider, C.W. (1997). Telomere shortening and tumor formation by mouse cells lacking telomerase DNA. Cell *91*, 25–34.

Bodmar, A.G., Frolkis, M., Chiu, C.-P., Morin, G.B., Harley, C.B., Shay, J.W., Lichtsteiner, S., and Wright, W.E. (1998). Extension of lifespan by introduction of telomerase in normal human cells. Science, in press.

Broccoli, D., Young, J.W., and de Lange, T. (1995). Telomerase activity in normal and malignant hematopoietic cells. Proc. Natl. Acad. Sci. USA *92*, 9082–9086.

Broccoli, D., Smogorzewska, A., Chong, L., and de Lange, T. (1997). Human telomeres contain two distinct Myb-related proteins, TRF1 and TRF2. Nature Gen. *17*, 231–235.

Cardenas, M.E., Bianchi, A., and de Lange, T. (1993). A Xenopus egg factor with DNA-binding properties characteristic of terminus-specific telomeric proteins. Genes Dev. *7*, 883–894.

Chong, L., van Steensel, B., Broccoli, D., Erdjument-Bromage, H., Hanish, J., Tempst, P., and de Lange, T. (1995). A human telomeric protein. Science *270*, 1663–1667.

Cooke, H.J., and Smith, B.A. (1986). Variability at the telomeres of the human X/Y pseudoautosomal region. Cold Spring Harbor Symp. Quant. Biol. *LI*, 213–219.

Counter, C.M., Avilion, A.A., LeFeuvre, C.E., Stewart, N.G., Greider, C.W., Harley, C.B., and Bacchetti, S. (1992). Telomere shortening associated with chromosome instability is arrested in immortal cells with express telomerase activity. EMBO J. *11*, 1921–1929.

de Lange, T. (1995). Telomere dynamics and genome instability in

human cancer. In Telomeres, E.H. Blackburn and C.W. Greider, eds. (Cold Spring Harbor, New York: Cold Spring Harbor), pp. 265–293.

de Lange, T. (1998). Telomeres and senescence: ending the debate. Science *279*, 334–335.

Dimri, G.P., Lee, X., Basile, G., Acosta, M., Scott, G., Roskelley, C., Medrano, E.E., Linskens, M., Rubelj, I., Pereira-Smith, O., et al. (1995). A biomarker that identifies senescent human cells in culture and in aging skin in vivo. Proc. Natl. Acad. Sci. USA *92*, 9363–9367.

Dionne, I., and Wellinger, R.J. (1996). Cell cycle-regulated generation of single-stranded G-rich DNA in the absence of telomerase. Proc. Natl. Acad. Sci. USA *93*, 13902–13907.

Farr, C., Fantes, J., Goodfellow, P., and Cooke, H. (1991). Functional reintroduction of human telomeres into mammalian cells. Proc. Natl. Acad. Sci. USA *88*, 7006–7010.

Garvik, B., Carson, M., and Hartwell, L. (1995). Single-stranded DNA arising at telomeres in cdc13 mutants may constitute a specific signal for the RAD9 checkpoint. Mol. Cell. Biol. *15*, 6128–6138.

Gossen, M., and Bujard, H. (1992). Tight control of gene expression in mammalian cells by tetracyclin-responsive promoters. Proc. Natl. Acad. Sci. USA *89*, 5547–5551.

Gottschling, D.E., and Zakian, V.A. (1986). Telomere proteins: specific recognition and protection of the natural termini of *Oxytricha* macronuclear DNA. Cell *47*, 195–205.

Hanish, J.P., Yanowitz, J., and de Lange, T. (1994). Stringent sequence requirements for telomere formation in human cells. Proc. Natl. Acad. Sci. USA *91*, 8861–8865.

Harley, C.B. (1995). Telomeres and aging. In Telomeres, E.H. Blackburn and C.W. Greider, eds. (Cold Spring Harbor, New York: Cold Spring Harbor), pp. 247–263.

Harley, C.B., Futcher, A.B., and Greider, C.W. (1990). Telomeres shorten during ageing of human fibroblasts. Nature *345*, 458–460.

Harlow, E., and Lane, D. (1988). Antibodies: A Laboratory Manual. (Cold Spring Harbor, New York: Cold Spring Harbor).

Hastie, N.D., Dempster, M., Dunlop, M.G., Thompson, A.M., Green, D.K., and Allshire, R.C. (1990). Telomere reduction in human colorectal carcinoma and with ageing. Nature *346*, 866–868.

Hayflick, L., and Moorhead, P.S. (1961). The serial cultivation of human diploid cell strains. Exp. Cell Res. *25*, 585–621.

Henderson, E. (1995). Telomere DNA structure. In Telomeres, E.H. Blackburn and C.W. Greider, eds. (Cold Spring Harbor, Cold Spring Harbor Press), pp. 11–34.

Kim, N.W., Piatyszek, M.A., Prowse, K.R., Harley, C.B., West, M.D., Ho, P.L.C., Coviello, G.M., Wright, W.E., Weinrich, S.L., and Shay, J.W. (1994). Specific association of human telomerase activity with immortal cells and cancer. Science *266*, 2011–2015.

Kirk, K.E., Harmon, B.P., Reichardt, I.K., Sedat, J.W., and Blackburn, E.H. (1997). Block in anaphase chromosome separation caused by a telomerase template mutation. Science *275*, 1478–1481.

Konig, P., and Rhodes, D. (1997). Recognition of telomeric DNA. Trends Biochem. Sci. *22*, 43–47.

Lansdorp, P.M., Verwoerd, N.P., van de Rijke, F.M., Dragowska, V., Little, M.-T., Dirks, R.W., Raap, A.K., and Tanke, H.J. (1996). Heterogeneity in telomere length of human chromosomes. Hum. Mol. Gen. *5*, 685–691.

Lin, J.-J., and Zakian, V.A. (1996). The Saccharomyces CDC13 protein is a single-strand TG1-3 telomeric DNA binding protein in vitro that affects telomere behavior in vivo. Proc. Natl. Acad. Sci. USA *93*, 13760–13765.

Linn, S.M., and Roberts, R.J. (1982). Nucleases. (Cold Spring Harbor, New York: Cold Spring Harbor Laboratory).

Makarov, V., Hirose, Y., and Langmore, J.P. (1997). Long G tails at both ends of human chromosomes suggest a C strand degradation mechanism for telomere shortening. Cell *88*, 657–666.

Marusic, L., Anton, M., Tidy, A., Wang, P., Villeponteau, B., and Bacchetti, S. (1997). Reprogramming of telomerase by expression of mutant telomerase RNA template in human cells leads to altered telomeres that correlate with reduced cell viability. Mol. Cell. Biol. *17*, 6394–6401.

McClintock, B. (1941). The stability of broken ends of chromosomes in zea mays. Genetics *26*, 234–282.

McClintock, B. (1942). The fusion of broken ends of chromosomes following nuclear fusion. Proc. Natl. Acad. Sci. USA *28*, 458–463.

McElligott, R., and Wellinger, R.J. (1997). The terminal DNA structure of mammalian chromosomes. EMBO J. *16*, 3705–3714.

Meyerson, M., Counter, C.M., Eaton, E.N., Ellisen, L.W., Steiner, P., Caddle, S.D., Ziaugra, L., Beijersbergen, R.L., Davidoff, M.J., Liu, Q., et al. (1997). hEST2, the putative human telomerase catalytic subunit gene, is up-regulated in tumor cells and during immortalization. Cell *90*, 785–795.

Morin, G.B. (1996). The structure and properties of mammalian telomerase and their potential impact on human disease. Semin. Cell Dev. Biol. *7*, 5–15.

Muller, H.J. (1938). The remaking of chromosomes. Collecting Net *13*, 181–195.

Nakamura, T.M., Morin, G.B., Chapman, K.B., Weinrich, S.L., Andrews, W.H., Lingner, J., Harley, C.B., and Cech, T.R. (1997). Telomerase catalytic subunit homologs from fission yeast and human. Science *277*, 955–959.

Nugent, C.I., Hughes, T.R., Lue, N.F., and Lundblad, V. (1996). Cdc13p: a single-strand telomeric DNA-binding protein with a dual role in yeast telomere maintenance. Science *274*, 249–252.

Price, C.M. (1990). Telomere structure in Euplotes crassus: Characterization of DNA-protein interactions and isolation of a telomere-binding protein. Mol. Cell. Biol. *10*, 3241–3431.

Saltman, D., Morgan, R., Cleary, M.L., and de Lange, T. (1993). Telomeric structure in cells with chromosome end associations. Chromosoma *102*, 121–128.

Sherwood, S.W., Rush, D., Ellsworth, J.L., and Schimke, R.T. (1988). Defining cellular senescence in IMR-90 cells: a flow cytomeric analysis. Proc. Natl. Acad. Sci. USA *85*, 9086–9090.

Smith, S., and de Lange, T. (1997). TRF1, a mammalian telomeric protein. Trends Genet. *13*, 21–26.

van Steensel, B., and de Lange, T. (1997). Control of telomere length by the human telomeric protein TRF1. Nature *385*, 740–743.

Wellinger, R.J., and Sen, D. (1997). The DNA structures at the ends of eukaryotic chromosomes. Eur. J. Cancer *33*, 735–749.

Wellinger, R.J., Wolf, A.J., and Zakian, V.A. (1993). Saccharomyces telomeres acquire single-strand $TG_{1\text{-}3}$ tails late in S phase. Cell *72*, 51–60.

Wright, W.E., Tesmer, V.M., Huffman, K.E., Levene, S.D., and Shay, J.W. (1997). Normal human chromosomes have long G-rich telomeric overhangs at one end. Genes Dev. *11*, 2801.

Yu, G.-L., Bradley, J.D., Attardi, L.D., and Blackburn, E.H. (1990). In vivo alteration of telomere sequences and senescence caused by mutated Tetrahymena telomerase RNAs. Nature *344*, 126–132.